J Pathol Inform

Editor-in-Chief:
Anil V. Parwani , Pittsburgh, PA, USA
Liron Pantanowitz, Pittsburgh, PA, USA

OPEN ACCESS
HTML format

For entire Editorial Board visit : www.jpathinformatics.org/editorialboard.asp

Symposium - Original Research

Atlas-guided correction of brain histology distortion

Xi Qiu[1,2,3], Lin Shi[2], Tony Pridmore[3], Alain Pitiot[3], Defeng Wang[2]

[1]Rotman Research Institute, University of Toronto, Canada, [2]Department of Imaging and Interventional Radiology, Chinese University of Hong Kong, China, [3]School of Computer Science, University of Nottingham, UK

E-mail: *Xi Qiu - nqiu@rotman-baycrest.on.ca
*Corresponding author

Received: 15 June 11 Accepted: 23 September 11 Published: 19 January 12

This article may be cited as:
Qiu X, Shi L, Pridmore T, Pitiot A, Wang D. Atlas-guided correction of brain histology distortion. J Pathol Inform 2011;2:S7.

Available FREE in open access from: http://www.jpathinformatics.org/text.asp?2011/2/2/7/92038

Abstract

Histological tissue preparation stages (e.g., cutting, sectioning, etc.) often introduce tissue distortions that prevent a smooth 3D reconstruction from being built. In this paper, we propose a method to correct histology distortions by running a piecewise registration scheme. It takes the information of several consecutive slices in a neighborhood into account. In order to achieve an accurate anatomic presentation, we run the method iteratively with the assistance from a pre-segmented brain atlas. The registration parameters are optimized to accommodate different brain sub-regions, e.g., cerebellum, hippocampus, etc. The results are evaluated by both visual and quantitative approaches. The proposed method has been proved to be robust enough for reconstructing an accurate and smooth mouse brain volume.

Key words: Piecewise image registration, Histology volume reconstruction, Histology distortion correction, Atlas-guided correction

Access this article online

Website: www.jpathinformatics.org

DOI: 10.4103/2153-3539.92038

Quick Response Code:

INTRODUCTION

Building and studying 3D representations of anatomical organs, such as the brain, plays an important role in modern biology and medical science. While 3D imaging methods such as MRI and CT provide accurate 3D structural information, 2D imaging methods such as histology and optical microscopy typically generate images with much higher resolution and better specific contrast. When studying the mouse brain, it is ideal to combine the advantages of both 3D and 2D imaging technologies. The classical approach is to reconstruct a 3D mouse brain volume from a series of histology slice images that provide more tissue details than MR images.[1-3] However, histology acquisition generally induces a lot of artifacts (holes, folding, tearing, sketching, etc.). Detecting and correcting the artifacts becomes a central issue when reconstructing a 3D volume from a series of histology slices. Indeed, they can make the distorted regions significantly different from the corresponding regions in adjacent slices. In a typical pairwise registration approach, artifacts lead to registration errors that tend to propagate to the adjacent slices through the slice-by-slice registration so that it prevents a smooth 3D brain volume from being reconstructed. Therefore, postacquisition distortion corrections are necessary.[1,2] As discussed, a conventional slice-by-slice 2D registration is not sufficient to correct the histology distortions.[4] In this case, 3D registration techniques can be employed to overcome the problem.[2,4-6]

Since studies in region of interest of mouse brain have been very popular in the past several decades, many 3D atlases are made available to support the research.[7-10] Mostly, they were acquired by one of the 3D imaging techniques (e.g., MRI, CT), and then manually segmented by biologists. The resolution of those atlases

varies a lot due to the different acquisition means and settings. The details of segmentations also differ a lot based on the degree of how small the functional regions in brain that the researchers required. Because the segmentation of the regions of interest in the atlas is reasonably closed to the ground truth,[2,11,12] it can be used as very supportive information to improve the quality and the accuracy of histological reconstruction.

A 3D volume reference acquired from the same brain of histology slices before sectioning would be perfect to correct the anatomically wrong information. However, such reference is not always available due to lack of equipment, limit of project, etc. While mouse brain anatomic atlas has been developed maturely, atlas from the same strain may not be the same individual as the histology sections, but still reasonably similar, hence can be used as a 3D volume reference. Moreover, atlases are well labeled with clear delineations of anatomical components that can lead us to correct the anatomical structures and shapes more locally and more purposefully.

Researchers have proposed approaches to detect distorted slices by evaluating the quality of image registration between slices.[5] Other methods[13,14] are based on the idea of eliminating the distorted slices rather than correcting them where possible. Quite often, most of serial histology slices have different types of distortions in different regions. If they are all removed, there may be not sufficient information left to reconstruct a 3D volume. A framework[15] was proposed to detect the distorted slices and predict the possible distorted structures while it may not be robust enough for a large amount of distortions. Therefore, we developed a method that takes more local information into account in a piecewise fashion and borrows information from a 3D atlas to improve the accuracy and robustness of distortion correction.

METHODOLOGY

Piecewise correction of histology distortion

Block-matching registration

In this method, we register histology slice S_i's neighbors located up to m slices away to itself using block-matching registration technique,[4] provided the slice thickness is small and even. Then, the local corresponding displacements $d_r^{j\to i}$ (r: region of interest; $j = i+n$; $n = 1,2, \ldots,m$) across those m slices are put together for comparison as shown in Figure 1. If the structure is not distorted and follows a smooth transition across several consecutive sections, the corresponding displacement vectors should have similar directional trends and similar lengths. However, if there is a structural distortion in at least one slice, the displacement vector of the distorted region in that slice will differ in direction and/or length from its counterpart vectors. Consequently, our target is to find those significantly different vectors so that we can have the knowledge of in which slice and where in that slice there may be a distortion, and also how the distortion may look like.

Displacement weighted-averaging

To make a fair comparison of the vectors, we employ a Gaussian filter to weight the distance n between the floating images and the reference image. The vector of interest receives the heaviest weight and the displacements of the corresponding regions in the neighboring slices receive smaller weights as their distance n to slice S_i increases, i.e.

$$w_g = g(n) = \frac{1}{\sqrt{2\cdot\pi}}\cdot e^{-\frac{n^2}{2\sigma^2}} \quad (1)$$

where σ is standard deviation of Gaussian distribution.

In addition to the Gaussian filter, averaged similarity measure CC (correlation coefficient) of the ROI has also been taken into account to weight the displacements. The regions that are more similar to the ROI receive higher weights, and vice versa:

$$\bar{d}_r^{\,j\to i} = \frac{\sum_{j=i+n}^{m} CC_r(j,i)\cdot d_r^{j\to i}}{\sum_{j=i+n}^{m} CC_r(j,i)} \quad (2)$$

where m is the number of the slices in this iteration.

Therefore, by combining the two terms of weights, we then derive a new set of displacements $d_r^{j\to i}$ for the ROI r as shown in Figure 1:

$$d_r^{*j\to i} = wg\cdot\bar{d}_r^{\,j\to i} = \frac{1}{\sqrt{2\cdot\pi}}\cdot e^{-\frac{n^2}{2\sigma^2}}\cdot\frac{\sum_{j=i+n}^{m} CC_r(j.i)\cdot d_r^{j\to i}}{\sum_{j=i+n}^{m} CC_r(j.i)} \quad (3)$$

Outlier detection using Z-score testing

Our outlier detection is based on standardized Z-score testing, i.e., $z = \frac{x-\mu_0}{\frac{\sigma}{\sqrt{n}}}$. Therefore,

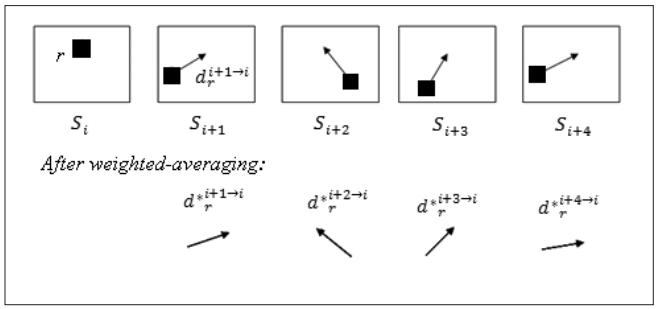

Figure 1: Displacements of the corresponding regions before and after weighted averaging

$$Z_r = \frac{T_r^i - \mu(T_r^{j\to i})}{\sigma(T_r^{j\to i})/\sqrt{m}} \quad (4)$$

where T_r^i is the transformation in region r at slice i; $u(T_r^{j\to i})$ and $\sigma(T_r^{j\to i})$ are the mean and the standard deviation of the displacements in region r at slice i to j, respectively.

In order to achieve good accuracy, we set the confidence level to 95%, and consequently, the Z = 1.64.

After the Z-score test, we identify the transformation that significantly differs from the others. Based on our theory, the ROI in that slice is very likely to be distorted. We should run our piecewise correction on that region.

Registration of outlier to nonoutlier regions

For every outlier region $r_{outlier}$ found in the last step, we apply the block-matching algorithm again to warp $r_{outlier}$ to its neighboring slices. For example, if S_{i+2} in Figure 1 is found to have outlier region, the estimated displacement for the outlier region is

$$d_{r_{outlier}} = wg \bullet \overline{d}_{r_{outlier}}^{i+2} = \frac{1}{\sqrt{2\bullet\pi}} \bullet e^{-\frac{n^2}{2\sigma^2}} \bullet \frac{\sum_{j=i+n}^{m} CC_r(j.i+2) \bullet d_r^{i+2}}{\sum_{j=i+n}^{m} CC_r(j.i+2)} \quad (5)$$

Here, we assume $dr_{outlier}$ is invertible, i.e. $dr_{outlier} = (\mathrm{d}r_{outlier}^{-1})^{-1}$

Therefore, by applying the inverted displacement to the outlier region, we make the outlier regions more similar to its nonoutlier neighbors, e.g., in Figure 2. We then implement this algorithm to every outlier region found within the slice neighborhood to correct histology distortions.

Our algorithm also runs iteratively to cover all the histology slices. In each iteration, we treat m consecutive slices $S_i \sim S_{i+m-1}$ as a registration neighborhood and choose the first slice of those m ones as the reference image. In the next iteration, neighborhood window shifts by one slice, i.e., $S_{i+1} \sim S_{i+m}$. By this way, every slice is treated as the reference of a group of consecutive slices to avoid reference bias.

Displacement regularization and filtering

Inevitably, a fair amount of outlier displacements might be generated by registration error. They may not match the anatomical features of interest adequately. An adaptive displacement regularization approach[16] estimates a rigid transformation within a predefined circular neighborhood cut to fit the local geometry around the region of interest and for each surrounding region that a displacement has been computed. Inhomogeneous displacements caused by registration error are regularized by this rigid transformation.

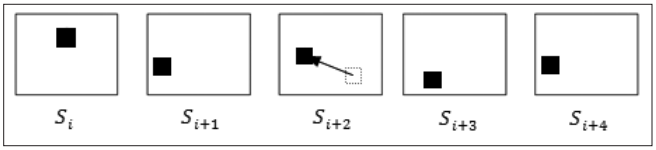

Figure 2: The distortion (dot-line square) in S_{i+2} is corrected by applying the inverted displacement of (5)

To make the whole displacement field even smoother, a mean filter is also applied in a circular neighborhood around every region of interest. The filter averages displacements in both x and y directions:

$$d(x,y) \to d'\left(\frac{1}{N}\sum_{j=1}^{N} x_j, \frac{1}{N}\sum_{j=1}^{N} y_j\right) \quad (6)$$

where j is the regions within the circular neighborhood around region of interest.

Finally, we warp every slice using the regularized and filtered displacement fields. All the corrected slices are then registered pair by pair to form a volume.

Atlas-guided anatomic structure recovery

A mouse brain has been reconstructed in the previous section. Nevertheless, the fact of lack of support and proof from a 3D ground truth still prevents the reconstructed volume from becoming a solid foundation for future studies. Therefore, a 3D reference is still necessary here for correcting the shape of reconstruction and, much expectantly, improving local smoothness as well. Consequently, we introduce a structural-improving technique of reconstructed volume guided by a presegmented 3D atlas of mouse brain. The already reconstructed volume is fused with the atlas. In each brain subregion, we further refine the parameters of our piecewise distortion correction method to achieve accurate brain structure and better volume smoothness.

Method framework

1. Register the 3D brain atlas of the same mouse strain to our reconstruction by the 3D fusion technique.[2]
2. Warp the atlas labels to the space of our reconstruction by the transformation of 1.
3. Label the brain regions in the reconstruction according to the warped atlas segmentation.
4. Refine the parameters for distortion correction to adapt the different brain regions.
5. Reconstruct a new volume using the refined parameters.

The method is operated in a coarse-to-fine fashion. The above steps are looped until a stopping criterion has been met. In the first iteration, a set of initial parameters is assigned for step 3. Those parameters are recommended as a prior knowledge by our neurologists based on the atlas. Thereafter, all the following iterations halve the parameters from the last iteration. We implement the method in this way to ensure the parameters can be optimized rapidly. The

stopping criterion is defined as an evaluation of mean smoothness[3] of the reconstructed volume, i.e., when mean smoothness measure $S_{k\leq 1}$, we stop the loop and output the reconstruction as the final result.

EXPERIMENTAL RESULTS

Experiment setup and parameters

In our experiment, a set of 350 Nissl-stained coronal images acquired by cyro-sectioning a single frozen C57BL/6J adult mouse brain from LONI Research Lab at the UCLA was used. Each image was sized to 900 × 900 pixels in a resolution of 10 μm per pixel during acquisition. The distance between the consecutive sections is 25 μm. In order to reduce the registration errors, we ran a prior step by applying a Gaussian filter (σ = 3) on the images to downsize them and reduce noise.

The computation of 87 iterations consumed a total ~40 hours, averaging ~15 minutes for the local correction of each slice. The block size of 1111, lattice site of every 10 pixels, and exploration neighborhood size of 71×71 were chosen, which was sufficient to cover the misaligning range for different slices in the dataset. Geometrical rigid regularization was applied on a circular range with a radius of 50 pixels and followed by an averaging filter with a radius of 20 pixels to optimize the raw displacement fields derived by the block-matching registration.

Based on the synthesized consideration of all the atlas' features,[2] the MR C57BL/6J Mouse Brain Atlas built by Brookhaven National Laboratory (BNL) was chosen as the 3D reference in our study.

2D correction results

The tuning regularization radius R (0~∞) will change the displacement field significantly. When R = 0, the geometrical regularization takes no effect on the displacement field, which equals a fully flexible transformation; whereas when R = ∞), a global rigid transformation will be yielded. As the R value becomes larger, the displacements become lighter and more evened out. Based on the resolution of our dataset and the minimum size of the topological texture we wanted to recover, we chose R=50 pixels as the radius of the regularization circular neighborhood.

After the displacement field had been calculated for outlier correction, we applied a serious of postprocessing steps to the displacement field in order. Parameters were regularization radius=50, averaging filter radius=20, and bilinear interpolation. Clearly, the corrected consecutive slices were locally aligned much better in details as highlighted in Figure 3. The better alignment would increase the reconstruction quality significantly.

3D reconstruction results

The chosen BNL atlas volume was registered to our reconstruction result from the method described in the Piecewise Correction of Histology Distortion section. The derived transformation was then applied to warp the atlas labels to the reconstruction. As Figure 4 shows, the main anatomical brain regions have been labelled in our reconstructed volume.

In our experiment, parameters were halved every iteration to quickly regress to the optimized combination. Table 1 shows the final set of the optimized parameters.

Table 1: The optimized parameters

	b_{size}	N_R	R_{Reg}	R_{Ave}	d_{Maj}
Cerebral cortex	15×15	40×40	50	30	3
Cerebellum	7×7	40×40	30	20	3
Midbrain	25×25	50×50	80	50	3
Thalamus	25×25	55×55	80	50	3
Corpus callosum	7×7	35×35	20	20	3
Hippocampus	5×5	25×25	15	15	3

b_{size}: block size, N_R: exploration neighborhood size, R_{Reg}: regularization radius, R_{Ave}: average filter radius, d_{Maj}: majority filter window.

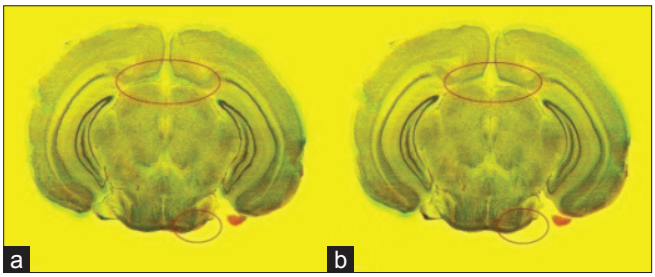

Figure 3: Distortion correction results in 2D: Two consecutive slices (no. 138 in red and no. 139 in green; perfect alignments: yellow) superimposed: (a) before and (b) after the piecewise distortion correction

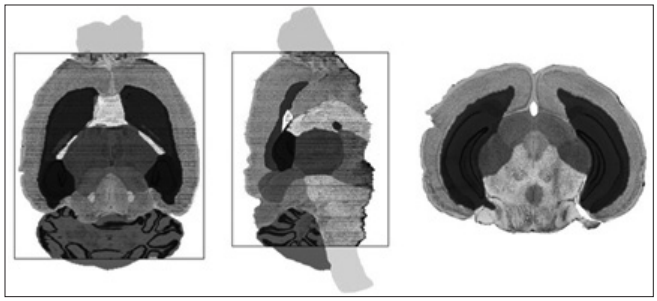

Figure 4: Warped atlas labels superimposed on top of the reconstructed volume

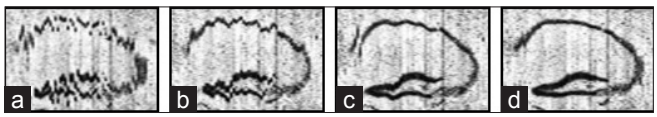

Figure 5: Hippocampus reconstructions in Sagittal view: (a) rigid-body alignment; (b) piecewise distortion correction only; (c) atlas-guided correction based on the initial parameters; (d) atlas-guided correction based on the optimized parameters

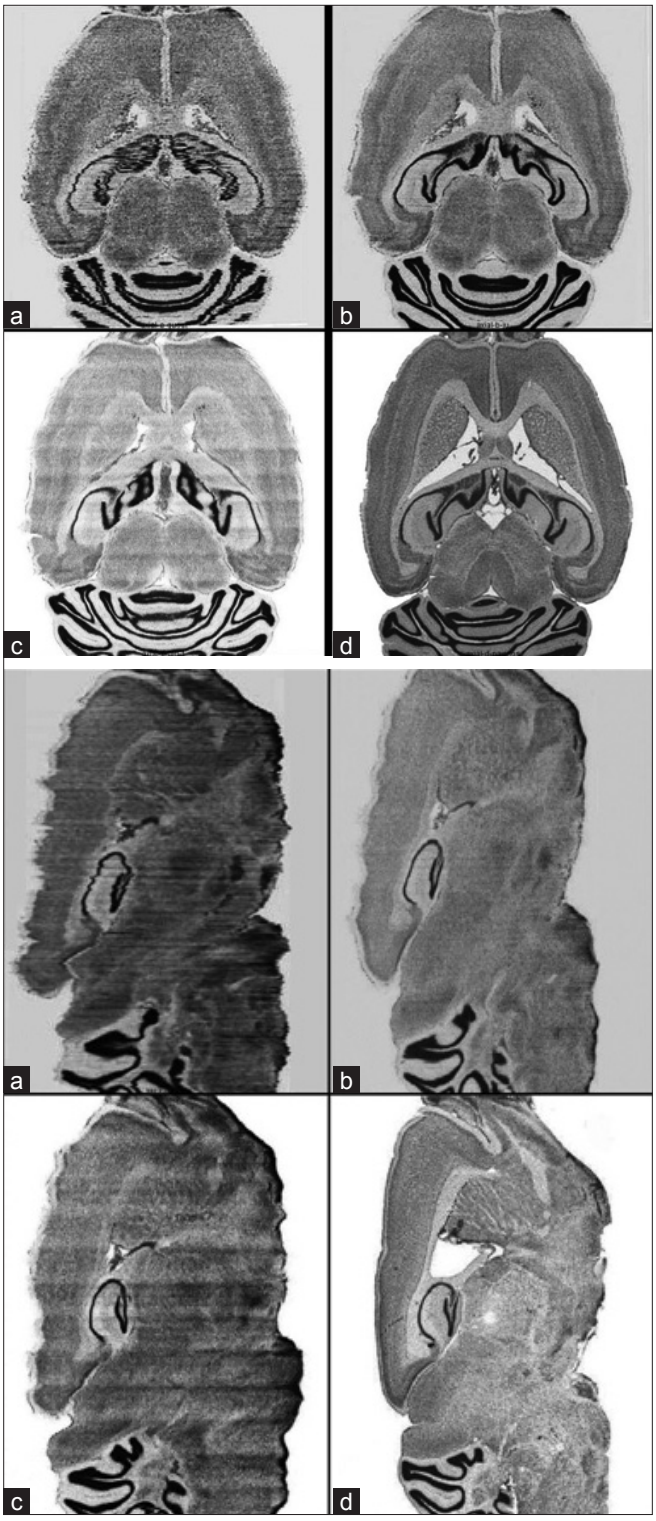

Figure 6: Result comparisons in axial and sagittal views: (a, b) reconstructed volume[3,18]; (c) our result; (d) no. 157 axial and no. 110 sagittal section of Paxino's atlas[10]

In Figure 5, the hippocampus reconstructed by the optimized parameters in Table 1 shows the accurate anatomic structure and the smoothest texture among the four.

A further noise removing tool – majority filter[17] – can be employed to ensure a smoother appearance of the reconstructed volume in the applications where intensity inhomogeneity is zero-tolerant, e.g., high-resolution visualization and atlas building.

To clearly show the advantages and the possible drawbacks of our atlas-guided scheme, we compared our results in Figure 6 (c) with Guest's (a), Ju's (b) corresponding views of results and also Paxino's histology atlas[10] as a reference.

Among the three sets of results, our reconstructed volume was noted that the inside anatomical features became a lot more coherent. Moreover, the result showed that the shapes of many key structures had been recovered thanks to the scheme of labeling out the brain regions and dealing with them in a respective manner. Our result was found to have more matches of anatomical regions with Paxino's atlas compared to either Guest's or Ju's results, in particular, hippocampus, corpus callosum, and cerebellum.

To evaluate the quality of smoothness achieved in our reconstructed volume, we employed a smoothness measure[3] S_k for every slice k as the following:

$$s_k = \frac{\sum_{i=0}^{n}\sum_{j=0}^{m}(B(i,j)+C(i,j)-2A(i,j))^2}{nm} \quad (7)$$

where $A(i,j)$ denotes the location of (i,j) in the warped image under evaluation; $B(i,j)$ and $C(i,j)$ denote the locations of the corresponding pixels of (i,j) on the two neighboring slices, respectively. S_k acts similar to the CAM measure.[18]

By the definition, S_k reflects the average distance from each pixel $A(i,j)$ to the mid-point of its two corresponding pixels in the consecutive slices, i.e.,

$$\frac{B(i,j)+C(i,j)}{2} \quad (8)$$

In other words, in the reconstructed volume, each pixel deviates averagely from the middle of its two corresponding pixels on the neighboring slices by $(B(i,j) + C(i,j)–2A(i,j))$ pixels.

To ensure that our reconstructed volume has achieved the satisfaction quantitatively, we computed a smoothness evaluation S_k which was also used as the stopping criterion in our iterative program. With the optimized parameters and majority filtering of three sections on each side, we achieved a reconstruction with a mean smoothness evaluation S_k = 0.92, i.e., in the reconstructed volume, on average, each point deviates from the middle of its two corresponding pixels on the neighboring sections by only about 0.46 pixel (9.8% closer than Ju's result: 0.51 pixel[3]).

DISCUSSION AND CONCLUSION

In this paper, we proposed a piecewise registration scheme and an atlas-guided anatomy recovery for mouse brain reconstruction. 2D distortions in histology slice were corrected in some degrees with the help from the undistorted information from the slice's neighbors. Presegmented atlas labels were firstly warped to the space of our reconstructed volume after the piecewise registration. Labeled anatomical regions in our reconstruction were then assigned an initial set of parameters of the piecewise registration and the optimization steps by neurologists based on the anatomical feature of the individual brain regions. Our automated framework was then operated to optimize the parameters iteratively by correcting local distortion piecewisely and rewarping the corrected sections pairwisely.

For result inspection, both visual and quantitative evaluations had been performed in comparison with other competitive approaches. Despite lacking global alignment in some regions compared to other methods due to the local nature of the atlas labels we referenced to, our results still showed clear advantages of local smoothness and better matching with the real histology sections over other methods in the comparison. Moreover, our method requires the least manual manipulation in the comparison.

In summary, our method has been proved as a reliable and robust way to correct distortions of local regions across consecutive histology sections and to subsequently reconstruct a smooth volume of mouse brain.

ACKNOWLEDGMENT

The work described in this paper was partially supported by a direct grant from CUHK Research Committee Funding, the Hong Kong Special Administrative Region, China (Project No.: MD10581).

REFERENCES

1. Ourselin S, Roche A, Subsol G, Pennec X, Ayache N. Reconstructing a 3D structure from serial histological sections. Image Vis Comput 2001;19;25-31.
2. Malandain G, Bardinet E, Nelissen K, Vanduffel W. Fusion of autoradiographs with an MR volume using 2-D and 3-D linear transformations. Neuroimage 2004;23:111-27.
3. Ju T, Warren J, Carson J, Bello M, Kakadiaris I, Chiu W, *et al*. 3D volume reconstruction of a mouse brain from histological sections using warp filtering. J Neurosci Methods 2006;156:84-100.
4. Pitiot A, Malandain G, Bardinet E, Thompson PM. Piecewise Affine Registration of Biological Images. In Proceedings of WBIR 2003. p. 91-101
5. Bardinet E, Ourselin S, Dormont D, Tandé D, Malandain G, Parain K, *et al*. Co-registration of histological, optical and MR data of the human brain. Med Image Comput Comput Assist Interv 2002;2488:548-55.
6. Ourselin S, Bardinet E, Dormont D, Malandain G, Roche A, Ayache N, *et al*. Fusion of Histological Sections and MR Images: Towards the Construction of an Atlas of the Human Basal Ganglia. In: Niessen WJ, Viergever MA, Editors, 4th Int. Conf. on Med Image Comput Comput Assist Interv, 2001;2208:743-51.
7. MacKenzie-Graham A, Lee EF, Dinov ID, Bota M, Shattuck DW, Ruffins S, *et al*. A multimodal, multidimensional atlas of the C57BL/6J mouse brain. J Anatomy 204;204:93-102.
8. Carson JP, Thaller C, Eichele G. A transcriptome atlas of the mouse brain at cellular resolution. Curr Opin Neurobiol 2002;12:562-5.
9. Sidman R. High Resolution Mouse Brain Atlas, available from: http://www.hms.harvard.edu/research/brain/atlas.html. [Last accessed on 2011]
10. Paxinos G, Franklin KB. The Mouse Brain in Stereotaxic Coordinates, 2nd ed. Waltham, Massachusetts: Academic Press; 2000.
11. Timsari B, Tocco G, Bouteiller J, Baudry M, Leahy R. Accurate registration of autoradiographic images of rat brain using a 3-d atlas. International Conference on Imaging Science, Systems, and Technology 1999.
12. Ali WS, Cohen FS. Registering coronal histological 2-D sections of a rat brain with coronal sections of a 3-D brain atlas using geometric curve invariants and B-spline representation. IEEE Trans Med Imaging 1998;17:957-66.
13. Yushkevich P, Avants B, Ng L, Hawrylycz M, Burstein P, Zhang H, *et al*. 3D Mouse Brain Reconstruction from Histology Using a Coarse-to-Fine Approach. Biomed Image Regist 2006. p. 230-7.
14. Tan Y, Hua J, Dong M. Feature Curve-guided Volume Reconstruction from 2D Images. 2007 4th IEEE International Symposium on Biomedical Imaging: From Nano to Macro., Arlington, VA, USA: 2007. p. 716-9.
15. Qiu X, Pridmore T, Pitiot A. Correcting Distorted Histology Slices for 3D Reconstruction. Med Image Underst Anal 2009.
16. Pitiot A, Guimond A. Geometrical regularization of displacement fields for histological image registration. Med Image Anal 2008;12:16-25.
17. Ju T, Warren J, Eichele G, Thaller C, Chiu W, Carson J. A geometric database for gene expression data. Symp Geom Process 2003;2003:166-76.
18. Guest E, Baldock R. Automatic reconstruction of serial sections using the finite element method. BioImaging. 1995;3;154-67.